中 文 摘 要

$Cu_{2.8}Mn_{0.2}Al$ 合金在淬火狀態下的顯微結構為 ($D0_3$+L-J) 相的混合。其中 $D0_3$ 相是在淬火中經由 $\beta \rightarrow B2 \rightarrow D0_3$ 之連續規律化的過程而來。此外，我們發現 L-J 相在 $\frac{a}{4}\langle 111\rangle$ 的反向晶界上比在 $\frac{a}{2}\langle 100\rangle$ 的反向晶界上更容易析出。當我們對此合金在 350℃至 750℃的溫度範圍內施以不同時間的時效處理後發現，此合金隨著溫度的增加其一系列相變化過程為 ($D0_3$ + L-J) → ($D0_3$ +L-J +γ_2) → (B2 +γ_2) → β；值得一提的是，在 Cu-Mn-Al 合金中，這一實驗結果從未被其他學者觀察過。此外，當此合金在 450℃作 16 小時的時效處理後，我們觀察到 γ_2 會在基地內析出；而隨著 γ_2 的成長，其周圍的錳含量也隨著增加，也因此促進 L-J 相在 γ_2 顆粒的周圍析出；這一實驗結果在 Cu-Mn-Al 合金中也從未被發現過。

Abstract

In the as-quenched condition, the microstructure of the $Cu_{2.8}Mn_{0.2}Al$ alloy was the mixture of ($D0_3$+L-J) phases and the $D0_3$ phase was formed by the β → B2 → $D0_3$ continuous ordering transition during quenching. Furthermore, it was found that the L-J precipitates are energetically more favorable to form at $\frac{a}{4}$<111> APBs than at $\frac{a}{2}$<100> APBs. When the as-quenched alloy was aged at temperatures ranging from 350℃ to 750℃, the phase transition sequence as the aging temperature increased was found to be ($D0_3$ + L-J) → ($D0_3$ +L-J +γ_2) → (B2 +γ_2) → β. It is noted here that this phase transition has never been observed by other workers in the Cu-Mn-Al alloys before. When the present alloy was aged at 450℃, γ_2 particles started to form within the $D0_3$ matrix. Along with the growth of the γ_2 particles, the surrounding region would be enriched in manganese. The enrichment of manganese would enhance the formation of the L-J precipitates at the regions contiguous to the

γ_2 particles. This feature has also never been reported by other workers in the Cu-Mn-Al alloys before.

Contents

List of figures

List of tables

Introduction

Phase transformations in $Cu_{3-x}Mn_xAl$ alloys have been extensively studied by many workers before[3-14]. Based on their studies, the $Cu_{3-x}Mn_xAl$ phase diagram with $0 \leqq X \leqq 1$ was established by M. Bouchard and G. Thomas, as shown in Figure 1. According to the phase diagram, it is seen that when the $Cu_{3-x}Mn_xAl$ alloy with $0.2 \leqq X \leqq 0.8$ was solution heat-treated at a point in the single β phase(disordered body-centered cubic) region and then quenched into iced brine rapidly, a $\beta \rightarrow B2 \rightarrow D0_3+L2_1$ transition would occur by an ordering transition and a spinodal decomposition during quenching. It means that the as-quenched microstructure of the $Cu_{3-x}Mn_xAl$ alloy with $0.2 \leqq X \leqq 0.8$ was a mixture of $(D0_3+L2_1)$ phases[8-22]. When the manganese content of the $Cu_{3-x}Mn_xAl$ alloy was increased to 25 atomic percent (X=1), the as-quenched microstructure of the alloy became a single $L2_1$ phase. The crystal structure of the $L2_1$ phase is similar to the $D0_3$ structure of the Cu_3Al[23-31]. The only difference between them is that the manganese atom replaced

the copper atom at a specific lattice site with eight nearest copper atoms in the $D0_3$ structure so as to form a stoichiometric composition of Cu_2MnAl[8], as shown in Figure 2[3].

In 1995, T. F. Liu and S. C. Jeng performed transmission electron microscopy observations on the phase transformation of a $Cu_{2.2}Mn_{0.8}Al$ alloy [2]. In their studies, it was found that a new type of precipitate (designated as L-J phase) with two variant could be observed within the ($D0_3$+$L2_1$) matrix in the as-quenched alloy. The L-J phase has an orthorhombic structure with lattice parameters a=0.413 nm, b=0.254 nm and c=0.728 nm. The orientation relationship between the L-J phase and the matrix was $(100)_{L\text{-}J}//(0\ \bar{1}\ 1)_m$, $(010)_{L\text{-}J}//(1\ \bar{1}\ \bar{1})_m$ and $(001)_{L\text{-}J}//(211)_m$. The rotation axis and rotation angle between two variants of the L-J phase were [021] and 90 deg. It was worthwhile to note here that the L-J phase had never been found previously by other workers in the Cu-Al, Cu-Mn and Cu-Mn-Al alloy systems.

When the as-quenched $Cu_{3-x}Mn_xAl$ alloys were aged at 700℃ or below for various times, three kinds of precipitates,

namely β-Mn, γ-brass and T-Cu_3Mn_2Al, were found in the $Cu_{3-x}Mn_xAl$ alloys. The β-Mn precipitate has an A13 (simple cubic) structure with lattice parameter a=0.641 nm[11]. The orientation relationship between A13 β-Mn and matrix was $(210)_{\beta\text{-Mn}}$ //$(100)_m$, $(\bar{1}20)_{\beta\text{-Mn}}$ //$(010)_m$ and $(001)_{\beta\text{-Mn}}$ //$(001)_m$ [32]. The γ-brass precipitate has a $D8_3$ (ordered body-centered cubic) structure with lattice parameter a=0.872 nm[10,11] and the orientation relationship between the γ-brass and the matrix was cubic to cubic[13,14]. The T-Cu_3Mn_2Al has a C15 structure with lattice parameter a=0.6903 nm[11,15,17].

To date, most of the studies are focused on the $Cu_{3-x}Mn_xAl$ alloy with $0.2 \leqq X \leqq 1$. Little information concerning the phase transformation in the $Cu_{3-x}Mn_xAl$ alloy with $X \leqq 0.2$ has been provided. Besides, in the $Cu_{3-x}Mn_xAl$ phase diagram (Figure 1), it is seen that the T_C ($\beta \rightarrow$B2) for the alloy with $X < 0.2$ is not quite sure. Therefore, the purpose of the present study is to examine the phase transformation of the $Cu_{2.8}Mn_{0.2}Al$ alloy by using transmission electron microscopy and energy dispersive X-ray spectrometer.

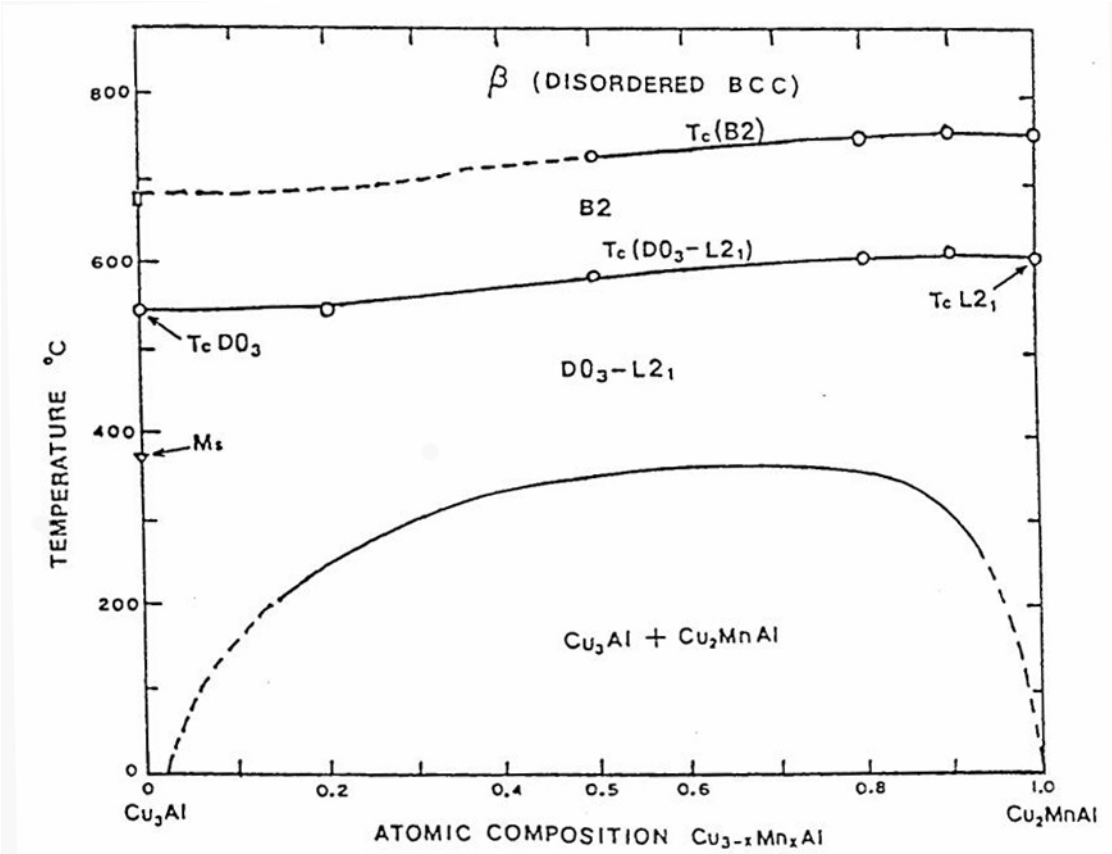

Fig. 1 A schematic drawing of the ordering temperatures T_C(B2) and T_C ($D0_3$+$L2_1$) and the miscibility gap of the $Cu_{3-x}Mn_xAl$ alloy.

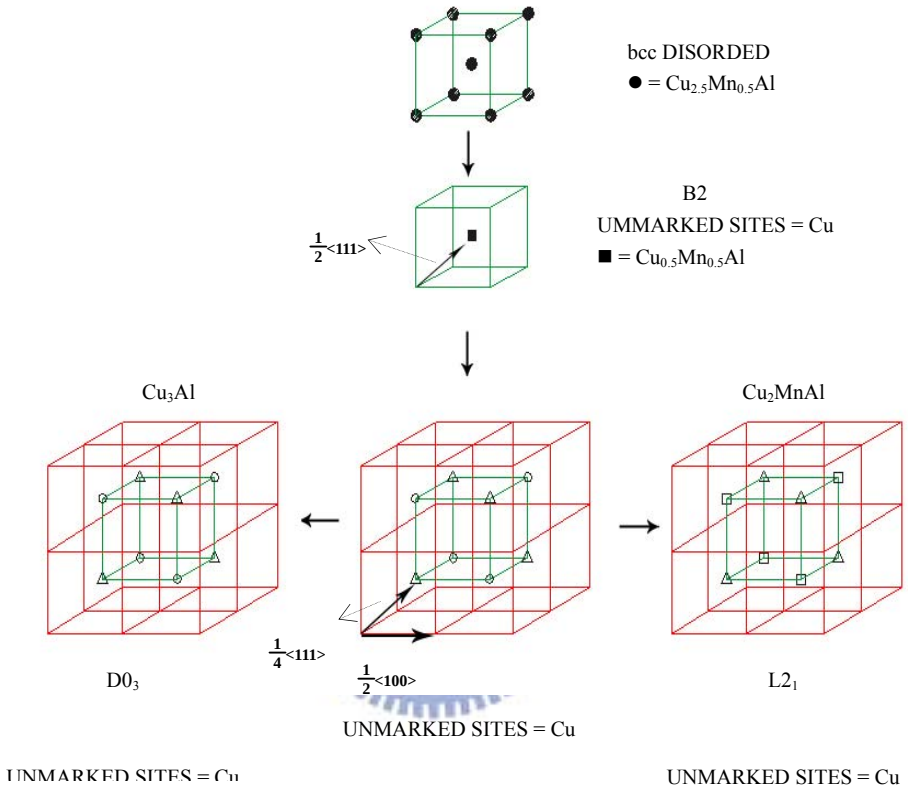

Fig. 2 Schematic representation of the ordering sequence of the quenched $Cu_{2.5}Mn_{0.5}Al$ alloy (vertically) and its isothermal decomposition (horizontally).

Experimental Procedure

(A) Alloy Preparation

The alloy, $Cu_{2.8}Mn_{0.2}Al$, was prepared in an air induction furnace by using 99.99 pct copper, 99.99 pct aluminum and 99.99 pct manganese. The melt was chill cast into a 30×50× 200-mm copper mold. After being homogenized at 850℃ for 72 hours under a protective argon atmosphere, the ingot was sectioned into 2.0 mm thick slices. The slices were subsequently solution heat-treated at 850℃ for 1 hour and rapidly quenched into iced brine. The aging processes were performed at the temperatures ranging from 350℃ to 750℃ for various times in a vacuum furnace and then quenched into iced brine rapidly .

(B) Transmission Electron Microscopy (TEM)

The electron microscopic specimens were prepared by means of a double jet electropolisher with an electrolyte of 70% methanol and 30% nitric acid. The polishing temperature was kept in the range from -40℃ to -30℃, and the current density

was kept in the range from 3.0×10^4 to 4.0×10^4 A/m^2. Electron microscopy was performed on a JEOL-2000FX scanning transmission electron microscope (STEM) operating at 200kV. This microscope was equipped with a Link ISIS 300 energy-dispersive X-ray spectrometer (EDS) for chemical analysis. Quantitative analyses of elemental concentrations for Cu, Al and Mn were made with the aid of a Cliff-Lorimer ratio Thin Section method.

Results

Figure 3 is a typical EDS spectrum of the as-quenched alloy. The quantitative analysis of ten different spectra indicated that the average chemical composition was Cu-(5 ± 0.3) wt pct Mn-(12.5±0.4) wt pct Al (Cu-(5±0.4) at pct Mn-(25±0.4) at pct Al). Figure 4 (a) is a bright-field (BF) electron micrograph of the as-quenched alloy, revealing the presence of the extremely fine precipitates within the matrix. Figures 4(b) through 4(d) are three selected-area diffraction patterns (SADPs) of the as-quenched alloy. It is seen that these SADPs consist of two sets of reflection reciprocal lattice : one derived from the matrix and another with streaks caused by the presence of the extremely fine precipitates (extra reflection spots indicated by arrows in the Figure 4(b)). Compared with our previous studies in $Cu_{2.2}Mn_{0.8}Al$ alloy and Cu-14.6Al-4.3Ni (wt%) alloy[2, 45] , it is seen that the extra reflection spots with streaks along <110> and <112> directions belong to the L-J phase with two variants[2]. The L-J phase has an orthorhombic structure with

lattice parameters a = 0.413nm, b = 0.254nm and c = 0.728nm, and the orientation relationship between the L-J phase and the matrix is $(100)_{L\text{-}J}//(0\bar{1}1)_m$, $(010)_{L\text{-}J}//(0\bar{1}\bar{1})_m$ and $(001)_{L\text{-}J}//(211)_m$. It is worthy to note here that the L-J phase has never been found by other workers in the Cu-Al, Cu-Mn and Cu-Mn-Al systems before. In addition to these extra reflection spots caused by the presence of the extremely fine L-J precipitates in Figures 4(b) through 4(d), all of the diffraction spots can be indexed as either the $D0_3$ or $L2_1$ phase, since both of these two phases possess the same arrangement of the reflection spots[3], and the difference between their lattice parameter is only about 2% (a = 5.95 Å in $L2_1$ phase and a = 5.83 Å in $D0_3$ phase) [34, 43]. However, the chemical composition of the present alloy approximates to Cu_3Al. Therefore, these diffraction patterns are considered to be of the $D0_3$ phase, rather than the $L2_1$ phase. Figure 4(e) is a (111) $D0_3$ dark-field (DF) electron micrograph of the same area as Figure 4(a), revealing the presence of the small $D0_3$ domains with $\frac{a}{2}$<100> anti-phase boundaries (APBs). Figure 4(f), a (200) $D0_3$ DF electron micrograph, shows the presence of the

B2 domains with the residual $\frac{a}{4}$<111> APBs. Therefore, it is deduced that the B2 and $D0_3$ domains were formed by the A2 → B2 → $D0_3$ continuous ordering transition during quenching[46-50]. Figure 4(g) is a DF electron micrograph taken with the reflection spot indicated by arrow marked as 〝1〞 in Figure 4(b), clearly exhibiting the presence of the extremely fine L-J precipitates. Based on the above observations, it is concluded that the microstructure of the as-quenched alloy is $D0_3$ phase containing extremely fine L-J precipitates, where the $D0_3$ phase was formed by the A2 → B2 → $D0_3$ continuous ordering transition during quenching.

Figure 5(a) is a BF electron micrograph of the present alloy aged at 350℃ for 24 hours and then quenched. It is seen that the presence of the large particles precipitate within the matrix. Figures 5(b) and 5(c), two SADPs, reveal that the arrangements of the reflection spots are similar to those observed in the as-quenched alloy. However the L-J precipitate reflection spots are much stronger than those of the as-quenched alloy. Figures 5(d) and 5(e) are the (111) and (200) $D0_3$ DF electron

micrographs of the same area as Figure 5(a), respectively. These figures show that a high density of the L-J precipitates (dark contrast) was present within the growth $D0_3$ domains. Figure 5(f) is a (100) L-J DF electron micrograph, exhibiting the coexistence of large and extremely fine L-J precipitates. This indicates that the microstructure of the alloy present at 350℃ was still a mixture of the ($D0_3$ +L-J) phases.

When the aging temperature was increased to 450℃, some irregular-like particles started to precipitate within the $D0_3$ matrix, as illustrated in Figure 6(a). Figure 6(b) and 6(c) are two SADPs taken from an area covering a irregular-like precipitate and its surrounding matrix. According to the camera length and the measurements of angles as well as d-spacings of the small diffraction spots, the crystal structure of the particle was determined to be an ordered body-centered cubic structure with lattice parameter a = 0.872 nm, which is consistent with that of the γ_2 phase [10, 11, 51, 52]. On the basis of these SADPs, it is found that the orientation relationship between the $D0_3$ matrix and the γ_2 precipitate is determined to be cubic to cubic. This

result is similar to that observed by other workers in the Cu-Mn-Al and Cu-Al-Ni alloys [13, 14]. Figure 6(d) is a (001) γ_2 DF electron micrograph, clearly showing the presence of the irregular-like γ_2 particles. Figures 6(e) and 6(f) are two SADPs taken from an area covering the L-J precipitates and their surrounding matrix. In these figures, it is clear that the L-J precipitate reflection spots are stronger than those of Figures 4(b) and 4(c). Figures 6(g) and 6(h) are (111) $D0_3$ and (100) L-J DF electron micrographs, clearly exhibiting the presence of the L-J precipitates within the $D0_3$ domains, respectively. Based on the above observations, it is concluded that the stable microstructure of the alloy aged at 450℃ was the mixture of ($D0_3$ + L-J + γ_2) phases.

Transmission electron microscopy examinations indicated that when the aging temperature was increased to 550℃, the stable microstructure was still a mixture of ($D0_3$ + L-J + γ_2) phases. However, when the alloy was aged at 650℃, the γ_2 particles were still observed. A typical example is illustrated in Figure 7(a), which is a BF electron micrograph of the alloy aged

at 650℃ for 2 hours and then quenched into iced brine. Figures 7(b) and 7(c) are two SADPs taken from the particle marked as 〝R〞 in Figure 7(a), indicating that the particle is also of γ_2 phase[10, 11, 51, 52]. Figure 7(d), an SADP taken from the matrix, shows that the microstructure was the mixture of ($D0_3$ + L-J) phases. Figure 7(e) and 7(f) are $(020)_1$ L-J and (111) $D0_3$ DF electron micrographs of the same area as Figure 7(a), exhibiting the presence of the L-J precipitates and small $D0_3$ domains, respectively. It is clear in Figures 7(e) and 7(f) that the sizes of both the L-J precipitates and $D0_3$ domains are similar to those of the as-quenched alloy. It is therefore reasonable to believe that these two phases were formed during quenching from the aging temperature; otherwise, their sizes should be increased at the aging temperature[46-50]. Figure 7(g), a (200) $D0_3$ DF electron micrograph, reveals that the B2 domains have grown to reach the whole grain and therefore no evidence of the $\frac{a}{4}$<111> APBs could be observed. This indicates that the microstructure of the matrix was the B2 phase. Based on the above observations, it is clear that the stable microstructure of the alloy

present at 650℃ was a mixture of (B2+ γ_2) phases.

When the aging temperature was increased to 750℃ and then quenched into iced brine, the microstructure of the alloy is similar to that of the as-quenched alloy. A typical example is shown in Figure 8. Figure 8(a) is a BF electron micrograph taken from the alloy aged at 750℃ for 1 hour. Figures 8(b) and 8(c), two SADPs, indicate that the microstructure present in Figure 8(a) is a mixture of the ($D0_3$ + L-J) phases. Figures 8(d) and 8(e) are $(020)_1$ L-J and (111) $D0_3$ DF electron micrographs of the same area as Figure 8(a). It is clearly seen that the L-J precipitates (dark contrast) within the $D0_3$ domains. Figure 8(f) is a (200) $D0_3$ DF electron micrograph, obviously showing the presence of the residual $\frac{a}{4}$<111> APBs within the B2 domains. This indicates that the microstructure existing at 750℃ or above was a single disordered β phase.

Based on the above experimental results, it is concluded that with increasing the aging temperature from 350℃ to 750℃, the phase transition sequence in the present alloy is ($D0_3$ + L-J) → ($D0_3$ +L-J + γ_2) → (B2 + γ_2) → β. The first transition

occurs between 350℃ and 450℃, the second between 550℃ and 650℃, and the third between 650℃ and 750℃.

Discussion

On the basis of the preceding results, some important experiment results are worthy to discuss as follows.

The effects of manganese content on the microstructure of the $Cu_{3-x}Mn_xAl$ alloy with $X > 0.2$ system have been extensively studied[2-18, 21,22]. Based on their studies, it was predicted that when the alloy was heat-treated at a point in the β phase-field and then quenched, a $\beta \rightarrow B2 \rightarrow D0_3$, $\beta \rightarrow B2 \rightarrow L2_1$ or $\beta \rightarrow B2 \rightarrow D0_3+L2_1$ ordering transition would occur during quenching. This means that both $\frac{a}{4}<111>$ and $\frac{a}{2}<100>$ -type APBs should be observed in the as-quenched alloy[4, 5, 23, 35]. However, to date, no evidence of the $\frac{a}{4}<111>$ -type APBs could be detected in the as-quenched alloy by transmission electron microscopy. The reason for the absence of the $\frac{a}{4}<111>$ APBs was proposed that the $\frac{a}{4}<111>$ APB energy in the Cu-Al-Mn and Cu-Al-Ni alloys is very high[3, 4, 44]. Therefore, the B2

domains would grow to reach the whole grains during quenching[4, 44]. However, the residual $\frac{a}{4}$<111> APBs should indeed be observed in the present as-quenched alloy. Comparing to previous studies[2-18, 21, 22], it seems to imply that the decrease of the manganese content could decrease the $\frac{a}{4}$<111> APB energy. Hence, the $\frac{a}{4}$<111> APBs became visible, as illustrated in Figure 4(f). In the as-quenched alloy, both the residual $\frac{a}{4}$<111> APBs and the small $D0_3$ domains with $\frac{a}{2}$<100> APBs could be observed. This result strongly confirmed that in the as-quenched alloy, the $D0_3$ phase was formed by the $\beta \rightarrow B2 \rightarrow D0_3$ continuous ordering transition during quenching.

In the present as-quenched alloy, it is seen that some fine L-J precipitates could be observed not only within the $D0_3$ matrix but also at $\frac{a}{4}$<111> and $\frac{a}{2}$<100> APBs, as shown in Figures 4(g) and 8(d) (as indicated by arrows), respectively. In these two figures, it is also seen that the sizes of the L-J

precipitates at $\frac{a}{4}$<111> APBs are larger than that at $\frac{a}{2}$ <100> APBs. This indicates that the L-J precipitates were formed preferentially at $\frac{a}{4}$<111> APBs than at $\frac{a}{2}$<100> APBs. Based on the previous studies[18, 24, 25], P. R. Swann also found the γ-brass formed preferentially at $\frac{a}{4}$<111> APBs than at $\frac{a}{2}$<100> APBs in an aged Cu-Ni-Al alloy[35]. G. Thomas et al. have reported that in a $Cu_{2.5}Mn_{0.5}Al$ alloy the energy of the $\frac{a}{4}$<111> APBs is 25% larger than the energy of the $\frac{a}{2}$<100> APBs, and the B2 ordering temperature is higher than the $D0_3$[3]. Therefore, it is reasonable to expect that the L-J precipitates are energetically more favorable to form at $\frac{a}{4}$ <111> APBs than at $\frac{a}{2}$<100> APBs.

When the as-quenched alloy was aged at 450℃, both of the γ-brass and the L-J precipitates could be observed within the matrix. That the size of the L-J precipitates contiguous to the

γ_2 particles is larger than that formed within the matrix is an important feature in the present study. In order to clarify this feature, an STEM-EDS study was used. Figures 9(a) and 9(b) represent two typical EDS spectra taken from a γ_2 particle and a L-J precipitate of the present alloy aged at 450℃ for 16 hour, respectively. The average atomic percentage of alloying elements examined by analyzing at least 10 different EDS spectra of each phase are listed in Table Ⅰ. For comparison, the chemical composition of the γ_2 particle and the L-J precipitate existing in the present alloy aged at 650℃ for 1 hour are also listed in Table Ⅰ. It is noted here that since in the present study the EDS analyses were made in the STEM mode on thin films (not on the extracted phase) and the size of the L-J precipitate (about 60nm) examined is slightly larger than that of the electron beam spot (40 nm) produced on the JEOL 2000FX STEM, some errors in the exact percentage of elemental concentrations in the L-J precipitates are in inevitable. However, it is seen that in Figure 9 and Table 1 the manganese concentrations in the L-J precipitates are greater than in the γ_2

particle, and the aluminum concentrations in the L-J precipitates are lower than in the γ_2 particle. Therefore, these analyses are still enough to permit an inference that the L-J precipitates are enriched in manganese and lacked in aluminum. On the basis of the above analyses, some discussions are appropriate. When the present alloy aged at 450℃, γ_2 particles started to precipitate within $D0_3$ matrix. Since the γ_2 particle is enriched in aluminum and lacked in manganese. Therefore it is to expect that along with the growth of γ_2 particles, the surrounding matrix would be enriched in manganese and lacked in aluminum. It seems to imply that increase of the manganese and decrease of aluminum would be enhanced the formation of the L-J precipitates. This result is consistent with the observation in Figure 6(h). In table 1, it is found that the concentration of aluminum in the L-J precipitates existing at 450℃ is lower than that at 650℃ and the concentration of manganese in the L-J precipitates existing at 450℃ is higher than that at 650℃. Based on the above analyses, it is thus to conclude that the size and the amount of the L-J precipitates existing at 450℃ are larger than those at

650℃.

It is worthwhile to mention here that in the present study, an attempt to determine the B2 → $D0_3$ ordering transition temperature was made. Figure 7(f) is a (111) $D0_3$ DF electron micrograph of the present alloy aged at 650℃ for 2 hours, revealing that the presence of the small $D0_3$ domains with $\frac{a}{2}$ <100> APBs. The $D0_3$ domain size is similar to that of the as-quenched alloy. However, the (200) $D0_3$ DF electron micrograph is all bright without the contrast of any $\frac{a}{4}$<111> APBs, as illustrated in Figure 7(g). This indicates that the B2 domain would grow to reach the whole grains at the aging temperature. Therefore, the stable microstructure of the present alloy at 650℃ is a mixture of (B2 + γ -brass) phases. It is thus concluded that the B2→$D0_3$ continuous ordering transition temperature is between 550℃ and 650℃.

Conclusions

1. The as-quenched microstructure of the $Cu_{2.8}Mn_{0.2}Al$ alloy was $D0_3$ phase containing extremely fine L-J precipitates. In the as-quenched alloy, both the large B2 domains with residual $\frac{a}{4}$<111> APBs and the small $D0_3$ domains with $\frac{a}{2}$<100> APBs could be observed. This result strongly demonstrated that the $D0_3$ phase was formed by the $\beta \rightarrow$B2 $\rightarrow D0_3$ continuous ordering transition during quenching.
2. When the present alloy was aged at 450℃ for 16 hours, γ_2 particles started to form within the $D0_3$ matrix. Along with the growth of the γ_2 particles, the surrounding region would be enriched in manganese. The enrichment of manganese would enhance the formation of the L-J precipitates at the regions contiguous to the γ_2 particles.
3. The B2$\rightarrow D0_3$ continuous ordering transition temperature is between 550℃ and 650℃
4. The $\beta \rightarrow$B2 continuous ordering transition temperature is

between 650℃ and 750℃.

5. The phase transition sequence as the aging temperature increased from 350℃ to 750℃ was found to be ($D0_3$+L-J) →($D0_3$+L-J+γ_2)→(B2+γ_2)→β.

References

1. K. C. Chu, S. C. Jeng and T. F. Liu : Scripta metal., 34, 83(1996).
2. S. C. Jeng and T. F. Liu : Metall Trans., 26A, 1353(1995).
3. M. Bouchard and G. Thomas : Acta Met., 23, 1485(1975).
4. Ye. G. Nesterenko, I. A. Osipenko and S. A. Fristov : Fiz. Metal. Metalloved., 27, 135(1969).
5. Ye.G. Nesterenko, I.A. Osipenko and S.A. Fristov : Fiz. Metal. Metalloved., 28, 987(1969).
6. Ye.G. Nesterenko, I.A. Osipenko and S.A. Fristov : Fiz. Metal. Metalloved., 36, 702(1973).
7. V.P. Zalutskiy, Ye.G. Nestenenko and I.A. Osipenko : Fiz. Metal. Metalloved., 28, 627(1970).
8. Ye.G. Nesterenko and I.A. Osipenko : Fiz. Metal. Metalloved., 36, 1212(1973).
9. R. Kozubski and J. Soltys : J. Mater. Sci. lett., 2, 141(1983).
10. B. Dubois and D.Chevereau : J.Mater. Sci., 14, 2992(1979).
11. R. Kozubski and J. Soltys : J.Mater. Sci., 17, 1441(1982).

12. R. Kozubski and J. Soltys : J.Mater. Sci., 14, 2296(1979).
13. R. Kozubski and J. Soltys : J.Mater. Sci., 18, 1689(1983).
14. T. Yamane, H. Okamoto and J. Takahashi : Z. Metallkde., 71, 813(1980).
15. R. Kozubski, J. Soltys and R. Kuziak : J. Mater. Sci.,18, 3079(1983).
16. R. Kozubski, J. Soltys, J. Dutkiewicz and J. Morgiel : J. Mater. Sci., 22, 3843(1987).
17. J. Soltys, M. Stefaniak and J. Holender : Phil. Mag., 49B, 151(1984).
18. D. R. F. West and D. Lloyd Thomas : J. Inst. Metals, 85, 97(1956-1957).
19. W. Koster and T. Godecke : Z. Metallk., 57, 889(1966)
20. B. G. Mellor, J. Hrenaze and C. Lopez del Castillo : Scripta Metall., 20, 839(1986).
21. C. Lopez del Castillo, J. Herenaze and B. G. Mellor : J. Mater. Sci., 4043(1986).
22. C. Lopez del Castillo, M. L. Blazouez, C. Gomez, B. G. Mellor, N. de Diego and J. del Rio : J. Mater. Sci.,

3379(1988).

23. M. G. Mendiratta, S. K. Ehlers and H. A. Lipsitt : Metall. Trans. A, 18A, 509(1987).
24. E. Persson : Z. physik, 57, 115(1929).
25. D. P. Oxley, R. S. Tebble and K. C. Williams : J. Appl. Phys., 34, 1362(1963).
26. W. Vandermeulen and A. Deruyttere : Metall. Trans., 4, 1659(1973).
27. D. Srivastava, P. Mukhopadhyay, E. Ramadasan and S. Banerjee : Metall. Trans. A, 24A, 495-501(1993).
28. W. G. Brammer, Jr. and C. G. Rhodes : Phil. Mag., 16, 477(1976).
29. G. B. Johnson and E. O. Hall : J. Phys. Chem. Sol., 9, 193(1968).
30. L. Arnberg and S. Westman : J. Appl. Cryst., 11, 148 (1978).
31. T. F. Liu and C. C. Wu : Scripta Metall., 23, 1243(1989).
32. K. C. Chu and T. F. Liu : Metall. Trans. A., 30, 1705(1999).
33. C. Goux, Bull. de Cercle d'Etudes des : Metaux, 8,

185(1961)

34. C. C. Wu, J. S. Chou and T. F. Liu : Metall. Trans. A., 22A, 1407(1991).
35. P. R. Swann : Phil. Mag., 14, 461(1966).
36. Y. Murakami, L. Delaey and G. S. Dullenkopf : Trans. JIM, 19, 317(1978).
37. K. Takezawa and S. Sato, J : Japan Inst. Metals, 37, 793(1973).
38. S. C. Jeng and T. F. Liu : Scripta Metall., 31, 665(1994).
39. M. De Bondt and A. Deruyttere : Acta Met., 15, 993(1967).
40. N. Kuwano and C. M. Waymam : Trans. Japan Inst. Metals., 24, 561(1983).
41. G. B. Johnson and E. O. Hall : J. Phys. Chem. Sol., 9, 193(1968).
42. L. Arnberg and S. Westmam : J. Appl. Cryst., 11, 148(1978).
43. Y. J. Chang : Acta metal., 30, 1185(1982).
44. N. Zárubová, A. Gemperle and V. Novák : Mater. Sci. Eng., A222, 166(1997).
45. J. Tan and T. F. Liu : Mater. Chem. Phys., 70, 49(2001).

46. J. W. Lee and T. F. Liu : Mater. Chem. Phys., 69, 192(2001).

47. P. R. Swann, W. R. Duff and R. M. Fisher : Metall. Trans., 3, 409(1972).

48. S. M. Allen and J. W. Cahn : Acta Metall., 24, 425(1976).

49. S. M. Allen : Phil. Mag., 36(1), 181(1977).

50. O. Ikeda, Y. Himuro, I. Ohnuma, R. Kainuma and K. Ishida : J. Alloys Comp., 268, 130(1998).

51. M. A. Dvorack, N. Kuwano, S. Polat, H. Chen and C. M. Wayman : Scripta Metall., vol 17, 1333(1983).

52. J. Singh, H. Chen and C. M. Wayman : Metall. Trans. A, vol 17A, 65(1985).

53. R. Kainuma, N. Satoh, X. J. Liu, I. Ohnuma and K. Ishida : J. Alloys Comp., 266, 191(1998).